Journal of Hazardous Materials 174 (2010) 236–243

Contents lists available at ScienceDirect

Journal of Hazardous Materials

journal homepage: www.elsevier.com/locate/jhazmat

Sensitivity and selectivity determination of BPA in real water samples using PAMAM dendrimer and CoTe quantum dots modified glassy carbon electrode

Huanshun Yin[a], Yunlei Zhou[a], Shiyun Ai[a,*], Quanpeng Chen[b], Xiangbin Zhu[b], Xianggang Liu[a], Lusheng Zhu[b,*]

[a] College of Chemistry and Material Science, Shandong Agricultural University, Daizong Street 61, Taian, 271018, Shangdong, China
[b] College of Resources and Environment, Shandong Agricultural University, Taian, 271018, Shandong, China

ARTICLE INFO

Article history:
Received 25 July 2009
Received in revised form 7 September 2009
Accepted 8 September 2009
Available online 16 September 2009

Keywords:
Bisphenol A
CoTe quantum dots
PAMAM dendrimer
Electrochemistry
Determination

ABSTRACT

Bisphenol A (BPA) is an environmental pollutant to disrupt endocrine system or cause cancer, thus the detection of BPA is very important. Herein, an amperometric sensor was fabricated based on immobilized CoTe quantum dots (CoTe QDs) and PAMAM dendrimer (PAMAM) onto glassy carbon electrode (GCE) surface. The cyclic voltammogram of BPA on the sensor exhibited a well-defined anodic peak at 0.490 V in 0.1 M pH 8.0 PBS. The determination conditions were optimized and the kinetic parameters were calculated. The linear range was 1.3×10^{-8} to 9.89×10^{-6} M with the correlation coefficient of 0.9999. The limit of detection was estimated to be 1×10^{-9} M. The current reached the steady-state current within about 5 s. Furthermore, the fabricated sensor was successfully applied to determine BPA in real water samples.

1. Introduction

Bisphenol A (BPA, 2,2′-bis(4-hydroxyphenyl)propane) is one of the endocrine disrupting compounds (EDCs), which mimics the action of hormone estrogen [1]. It is found that BPA could also possibly cause cancer, and an association between BPA and breast cancer has been discovered [2]. These findings are particularly important, because BPA is a monomer for the production of polycarbonate (PC), a stabilizing material of polyvinyl chloride (PVC) and a major component of epoxy resin (EP), which are widely employed for nursing bottle, food can lining and beverage container, from which BPA can leach into food and environment, especially at elevated temperatures, for extending periods of time [3–5]. In addition, several reports have also demonstrated that BPA can also migrate into agriculture soil [6], lake water [7] and river water [8] from the plastic manufacturing process or the degradation product of plastic. Therefore, quantitative determination of BPA by reliable and fast method is necessary for the trace level environmental contamination.

Various methods, such as high-performance liquid chromatography (HPLC), liquid chromatography–mass spectrometry (LC–MS), liquid chromatography with electrochemical detector (LC-ED), gas chromatography–mass spectrometry (GC–MS), fluorimetry, enzyme-linked immunosorbent assay (ELISA) and molecular imprinting technique [9,10] have been reported for determination of BPA. Apart from those methods, electrochemically analytical technique has great potential for environmental monitoring because of its fast response speed, cheap instrument, low cost, simple operation, timesaving, high sensitivity, excellent selectivity and real-time detection in situ condition. BPA could be oxidized at electrode surface due to containing phenolic hydroxyl groups [11–15]. However, direct detection of BPA using bare electrode is rare, because the response of BPA is poor and the oxidation of BPA always involves a relatively high overpotential [11]. Thus, the application of bare electrode for BPA detection is limited. In order to settle these problems, chemically modified electrodes have been developed. Furthermore, modification of electrode surface can provide a way to extend the dynamic range in analytical determination [16]. Therefore, novel electrode modification material with high sensitivity, catalytic activity and conductivity should be developed.

Quantum dots (QDs), also called semiconductor nanocrystals, are a class of nanoparticles containing group II–VI elements or group III–V elements, with diameter between 1 and 100 nm. Due to their size-tunable, chemically functionalizable surface, electronic property and catalytic effect, they are widely used as modified material in electrochemical sensors. For example, Wang et al. reported a H_2O_2 sensor based on incorporated horseradish peroxidase (HRP) and liophilic CdS/ZnS QDs onto the surface of GCE [17]. Liu et al. constructed a novel electrochemical biosensing platform of glucose by modifying a GCE with glucose oxidase, CdTe QDs and CNTs [18]. Dendrimers belong to a new class of synthetic

* Corresponding authors. Tel.: +86 538 8247660; fax: +86 538 8242251.
E-mail addresses: ashy@sdau.edu.cn (S. Ai), lushzhu@sdau.edu.cn (L. Zhu).

0304-3894/$ – see front matter © 2009 Elsevier B.V. All rights reserved.
doi:10.1016/j.jhazmat.2009.09.041

macromolecule, which possess a regularly branched treelike structure. In recent years, poly(amidoamine) (PAMAM) dendrimers have attracted more attention because of their high geometric symmetry, easily controlled nanosize, controllable surface functionality, film forming ability and chemical stability [19–21]. Moreover, PAMAM could be easily protonated to make external amino-groups positively charged in neutral and alkaline conditions [22], which would be applied to adsorb the negatively charged BPA.

To the best of our knowledge, electrode modified with CoTe QDs has not yet been reported. Therefore, this paper describes a simple method based on immobilized fourth-generation (G4) PAMAM dendrimer and CoTe QDs on glassy carbon electrode (GCE) using layer-by-layer assembly technique for the determination of trace amounts of BPA. The effect factors were optimized and the kinetic parameters were calculated. The sensitivity, linear range, limits of detection and stability of the prepared electrochemical sensor in the detection of BPA were also investigated.

2. Experiments

2.1. Reagents and apparatus

Amine terminated G4 poly(amidoamine) dendrimer (G4 PAMAM) and BPA was purchased from Aldrich Chemical Co. (USA). 0.1 M BPA stock solution was prepared with anhydrous ethanol and kept in darkness at 4°C in a refrigerator. Working solutions were freshly prepared before use by diluting the stock solution. 0.4 mM PAMAM solution was prepared with methanol. CoTe QDs were prepared according to the previous report [23]. Phosphate buffer solution (PBS) was prepared by mixing stock solutions of 0.1 M NaH_2PO_4 and 0.1 M Na_2HPO_4 and adjusting the pH with 0.1 M H_3PO_4 or 0.1 M NaOH. $CoSO_4{\cdot}7H_2O$, TeO_2, ethanolamine, glucose and other reagents were of analytical reagent grade and used as received without further purification. All the solutions were prepared with redistilled deionized water from quartz.

Electrochemical experiments were performed with CHI660C electrochemical workstation (Shanghai Chenhua Co., China) with a conventional three-electrode cell. A bare or modified GCE was used as working electrode. A saturated calomel electrode (SCE) and a platinum wire were used as reference electrode and auxiliary electrode, respectively. The pH measurements were carried out on PHS-3C exact digital pH meter (Shanghai KangYi Co. Ltd., China), which was calibrated with standard pH buffer solutions. All the measurements were carried out at 25 ± 0.5 °C.

2.2. Preparation of PAMAM/CoTe/GCE

Before modification, a bare GCE (3 mm in diameter) was polished to a mirror-like with 0.3 and 0.05 μm alumina slurry on micro-cloth pads, rinsed thoroughly with redistilled deionized water between each polishing step, then washed successively with redistilled deionized water, anhydrous alcohol and redistilled deionized water in an ultrasonic bath and dried in air before use.

For preparation of PAMAM/CoTe/GCE, 1 mg mL^{-1} CoTe solution was first prepared with redistilled deionized water, followed by ultrasonication for 30 min to obtain a homogeneously dispersed solution. With a microinjector, 5 μL of CoTe suspension was deposited on the fresh prepared electrode surface. After the solvent was evaporated, the electrode surface was thoroughly rinsed with redistilled deionized water and dried in air. Then, 5 μL PAMAM solution (0.4 mM) was dropped onto the surface of CoTe/GCE. (To obtain good cyclic voltammetric response of the PAMAM/CoTe/GCE, the amounts of CoTe and PAMAM were optimized in control experiments and finally the above loadings were chosen.) After dried under ambient condition, the modified electrode was wasted with redistilled deionized water to remove the unimmobilized modifier. The obtained electrode was noted as PAMAM/CoTe/GCE. For comparison, CoTe/GCE and PAMAM/GCE were fabricated with similar procedures. All the modified electrodes were stored at 4 °C in a refrigerator before use.

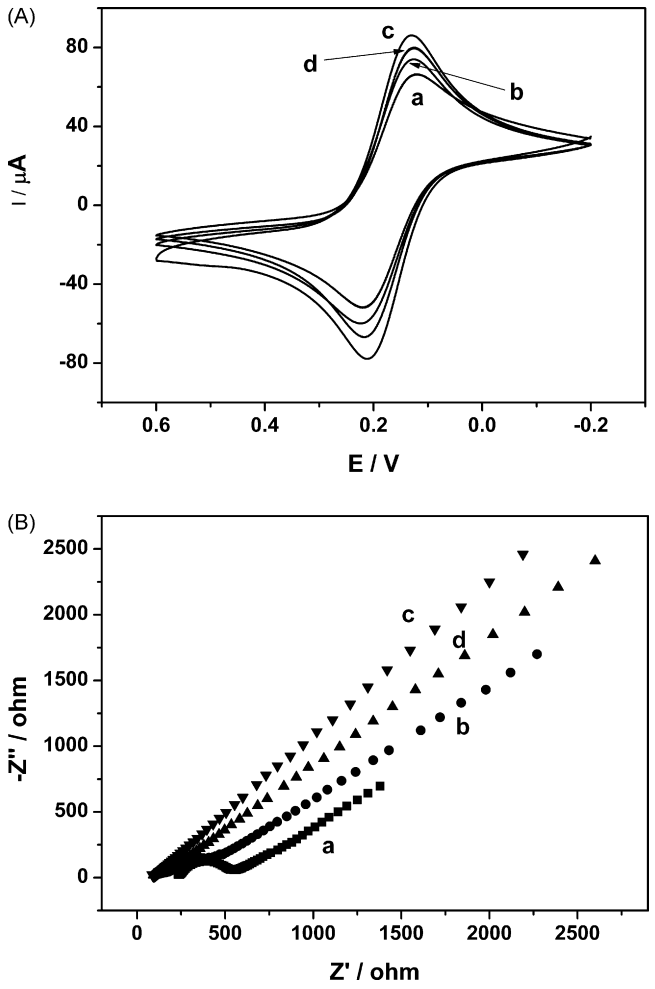

Fig. 1. Cyclic voltammograms (A) and Nyquist plots (B) of different electrodes in 5 mM $Fe(CN)_6^{3-/4-}$ (1:1) solution containing 0.1 M KCl. Scan rate: 100 mV s^{-1}. The frequency range was from 0.1 to 10^5 Hz at the formal potential of 0.17 V. (a) GCE, (b) CoTe/GCE, (c) PAMAM/GCE and (d) PAMAM/CoTe/GCE.

3. Results and discussion

3.1. Characterization of electrochemical behavior of PAMAM/CoTe/GCE

Cyclic voltammetric responses at bare electrode and different modified electrodes in 5 mM $Fe(CN)_6^{3-/4-}$ were shown in Fig. 1A. Curve 'a' was cyclic voltammogram of GCE with peak-to-peak separation (ΔE_p) of 103 mV. Curve 'b' and curve 'c' were cyclic voltammograms of CoTe/GCE and PAMAM/GCE with ΔE_p of 96 and 81 mV, respectively. Compared with bare electrode, the peak currents of CoTe/GCE and PAMAM/GCE increased dramatically and the ΔE_p decreased obviously, indicating that CoTe QDs and PAMAM could greatly increase the electron transfer rate of $Fe(CN)_6^{3-/4-}$, respectively. This phenomenon could be attributed to the huge surface area of CoTe and the electrostatic adsorption between the positively charged surface confined PAMAM molecule and the negatively charged $Fe(CN)_6^{3-/4-}$ probe. When PAMAM-CoTe was deposited on GCE surface, the peak currents decreased and ΔE_p

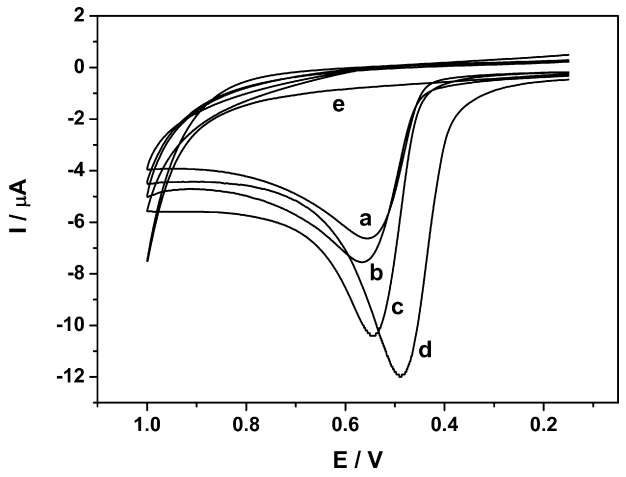

Fig. 2. Cyclic voltammograms of 0.25 mM BPA at GCE (a), CoTe/GCE (b), PAMAM/GCE (c) and PAMAM-CoTe/GCE (d) in 0.1 M PBS (pH 8). (e) PAMAM/CoTe/GCE in blank PBS. Scan rate: 100 mV s^{-1}. Accumulation time: 240 s.

increased to 84 mV compared with PAMAM/GCE, which might be caused by the semi-conductive property of CoTe.

For further characterization of the modified electrode, electrochemical impedance spectroscopy (EIS) was used. Fig. 1B showed Nyquist diagrams of 5 mM $[Fe(CN)_6]^{3-/4-}$ in 0.1 M KCl at different electrodes. Curve 'a' was Nyquist diagram of GCE. In the high frequency section, a big well-defined arc was observed, indicating a huge interface electron transfer resistance. The resistance value decreased after the bare electrode was modified with CoTe (curve b). When PAMAM was immobilized on GCE surface, a nearly straight line was observed (curve c), indicating a very small interfacial electron transfer resistance. The positively charged PAMAM molecule has a three-dimensional spherical structure and a large specific surface area, which could significantly increase the electrode surface area, effectively attract negatively charged $Fe(CN)_6^{3-/4-}$. Thus, the interface electron transfer resistance was decreased, and the electron transfer rate could be improved. When PAMAM-CoTe was deposited on GCE, the interfacial electron transfer resistance increased a little, which could be attributed to the existence of CoTe with semiconductor properties. This result also demonstrated that PAMAM-CoTe was successfully immobilized on the GCE surface.

3.2. Cyclic voltammetric behaviors of BPA

Fig. 2 showed cyclic voltammograms of GCE (a), CoTe/GCE (b), PAMAM/GCE (c) and PAMAM/CoTe/GCE (d and e) in the presence (a–d) and absence (e) of 0.25 mM BPA in 0.1 M pH 8.0 PBS. There was no redox peak obtained at PAMAM/CoTe/GCE without BPA, indicating the PAMAM-CoTe composite film was non-electroactive in the selected potential region. When 0.25 mM BPA was added, an well-defined oxidation peak was observed during the sweep from 0.20 to 1.00 V at all the electrodes. However, no corresponding reduction peaks were observed. It suggests that the electrode response of BPA is a typical of totally irreversible electrode reaction, which is in accordance with other reports [11,12,24–28]. Both the oxidation currents of BPA at CoTe/GCE and PAMAM/GCE increased when comparing with GCE, which could be attributed to the favorable catalytic activity of CoTe and electrostatic adsorption between positively charged PAMAM and negatively charged BPA. G4 PAMAM possesses 64 primary amine groups which can be easily protonated in alkalescent condition [22]. Therefore, that is in favor of adsorption of BPA with negative charge to enhance the current response. When PAMAM-CoTe was immobilized on the surface of GCE, the oxidation current further increased and the oxidation potential shift more negatively, which might be attributed to the synergetic activity of PAMAM and CoTe. In other words, the negative potential shift indicates the significant electrocatalytic activity of the modified electrode, and the current increase could be attributed mainly to a surface accumulation ability of the modified layer resulting from the protonated PAMAM [19]. The extraordinarily electrocatalytic activity of CoTe-PAMAM may be attributed to the small dimension effect, quantum size effect, the large specific surface area, the distinctive electronic characteristics, the high adsorption capacity and the excellent electron transfer ability, which lead to the larger electroactive surface of the modified electrode for the detection of BPA [17–19,29].

The oxidation peak potential of BPA at PAMAM/CoTe/GCE (0.490 V) was smaller than some of previous reports in near-neutral pH conditions, such as Si/boron-doped electrode (1.2 V, vs. SCE) [30], carbon paste electrode (0.89 V, vs. SCE) [24], Pt electrode (about 0.74 V, vs. Ag/AgCl) [25], glassy carbon electrode (0.65 V, vs. Ag/AgCl [26]) CNT/GCE (0.59 V, vs. Ag/AgCl) [27] and carbon-felt electrode (0.54 V, vs. Ag/AgCl) [28]. Therefore, a substantial decrease in oxidation overpotential has been achieved in the present study with PAMAM/CoTe/GCE. However, the oxidation peak potential of BPA in this work was a little bigger than that at CoPc-CPE (0.454 V vs. SCE) [12]. The difference of oxidation potential of BPA might be attributed to the electrolyte, matrix electrode, modification procedure and modification material.

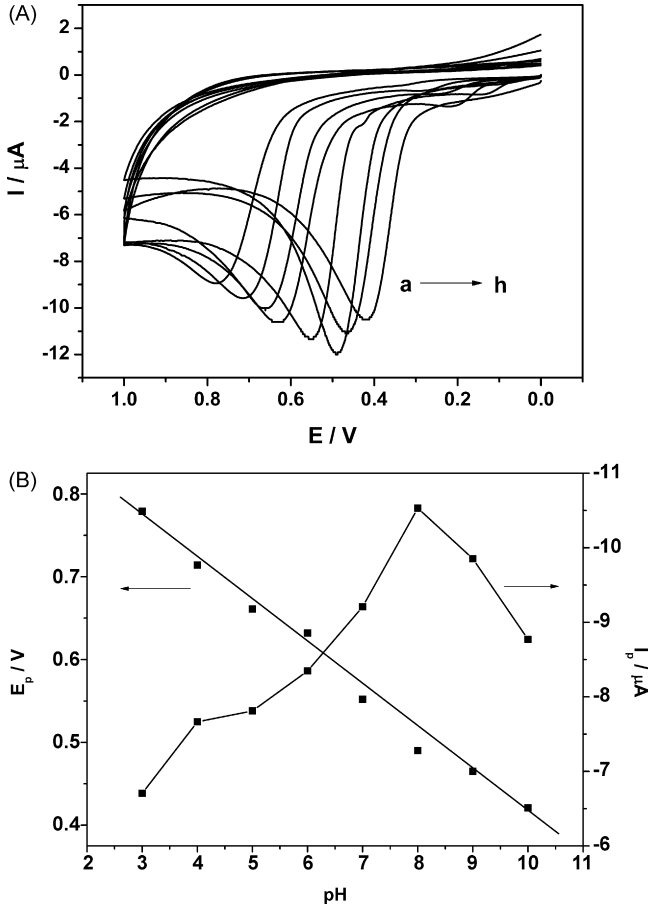

Fig. 3. (A) Cyclic voltammograms of 0.25 mM BPA at PAMAM/CoTe/GCE with different pH. (a–h) 3, 4, 5, 6, 7, 8, 9 and 10. (B) Effects of pH on the current response and potential response. Other conditions are the same as in Fig. 2.

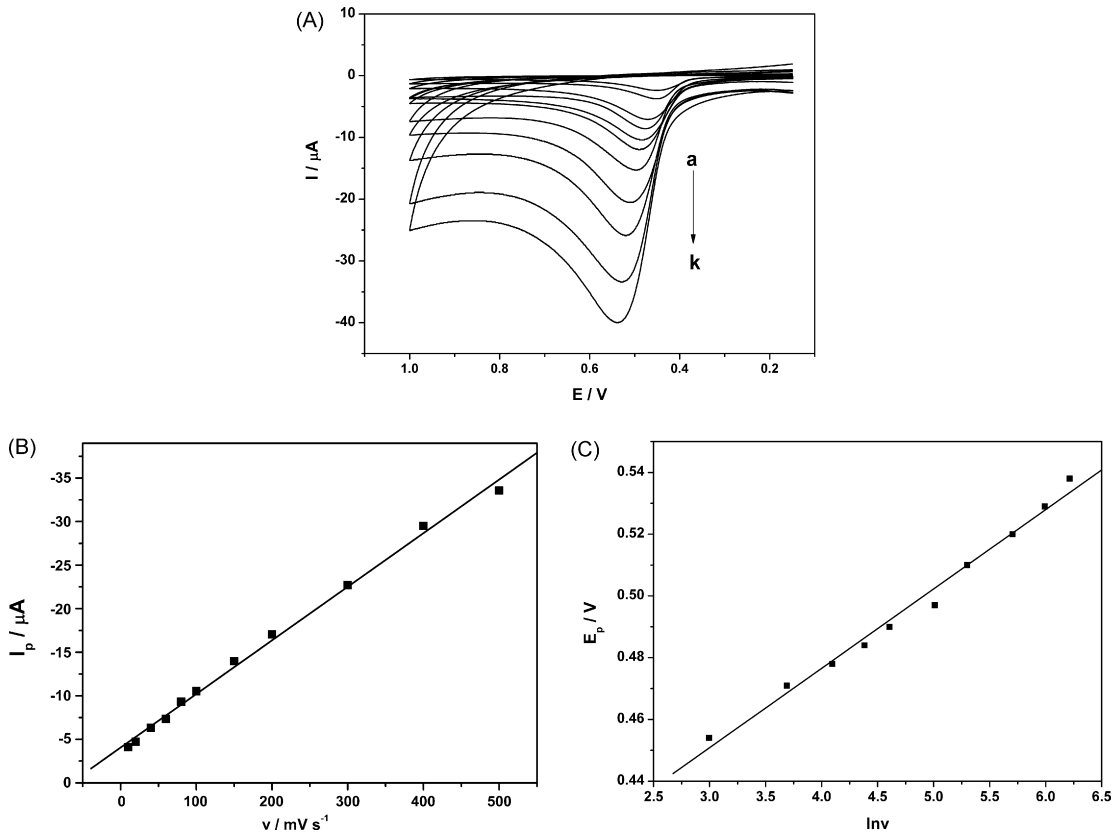

Fig. 4. (A) Cyclic voltammograms of 0.25 mM BPA at PAMAM/CoTe/GCE with different scan rates. Curves (a–k) are obtained at 10, 20, 40, 60, 80, 100, 150, 200, 300, 400 and 500 mV s^{-1}, respectively. (B) The plot for the dependence of peak current on scan rate. (C) The relationship between E_{pa} and ln v. Other conditions are the same as in Fig. 2.

3.3. Effect of pH

The effect of solution pH on the oxidation of 0.25 mM BPA at PAMAM/CoTe/GCE was investigated in the pH range from 3.0 to 10.0 by cyclic voltammetry (Fig. 3A). As shown in Fig. 3B, the oxidation peak current gradually increased with an increasing pH value from 3.0 to 8.0. Then the oxidation peak current decreased when the solution pH exceeded 8.0. The primary amine groups in different generations of PAMAM could be completely protonated to make external amino-groups positively charged at a certain pH, and then the protonation level of PAMAM would decrease with pH further increasing [22]. Therefore, based on previous report [22] and the results obtained from this work, we think that the G4 PAMAM on the electrode surface would be completely protonated at about pH 8.0, which could be used to adsorb the negatively charged BPA to obtain the maximum current response. Then, when pH was larger than 8.0, the protonation level of G4 PAMAM would decrease, which could reduce the BPA adsorbance, leading to decrease the current response. Considering the sensitivity of the determination of BPA, a pH of 8.0 was chosen for the subsequent analytical experiments. The relationship between the oxidation peak potential (E_{pa}) and pH was also shown in Fig. 3B. A linear shift of E_{pa} towards negative potential with an increase of pH indicated that protons were directly involved in BPA oxidation, and that it obeyed the following equation: E_{pa} (V) = −0.052 pH + 0.9242 (R = 0.9954). A slope of 0.052 V pH^{-1} is approximately close to the theoretical value of 0.0576 V pH^{-1}, indicating that the electron transfer is accompanied by an equal number of protons in electrode reaction [31].

3.4. Effect of scan rate

As shown in Fig. 4A, the effect of scan rate (v) on the oxidation of BPA was investigated by cyclic voltammetry. A linear relationship of peak current versus scan rate was obtained in the range from 10 to 500 mV s^{-1} (Fig. 4B). Such behavior suggests that the oxidation of BPA at PAMAM/CoTe/GCE is a typical adsorption-controlled electrode process. Moreover, a linear correlation of E_{pa} versus ln v was observed with a slope of 0.026 (shown in Fig. 4C). As for an adsorption-controlled and totally irreversible electrode process, according to Laviron, E_{pa} is defined by the following equation [32]:

$$E_{pa} = E^0 + \left(\frac{RT}{\alpha nF}\right) \ln\left(\frac{RTk^0}{\alpha nF}\right) + \left(\frac{RT}{\alpha nF}\right) \ln v \quad (1)$$

where α is transfer coefficient, k^0 is standard rate constant of the reaction, n is electron transfer number involved in rate-determining step, v is scan rate, and E^0 is formal redox potential. Other symbols have their usual meanings. Thus, the value of αn can be easily calculated from the slope of E_{pa} versus ln v. In this work, the slope is 0.026, therefore, αn is calculated to be 0.999. Generally, α is assumed to be 0.5 in totally irreversible electrode process. So, the electron transfer number (n) is 2. In Section 3.3, it is demonstrated that the number of electrons and protons involved in the oxidation process is equal. Therefore, the electrooxidation of BPA on PAMAM/CoTe/GCE is a two-electron and two-proton process.

According to previous reports with regard to the oxidation of BPA and other phenolic compounds [26,33–36] and the results obtained from this work, the electrochemical oxidation mechanism of BPA can be expressed as follows (Scheme 1).

It is well-known that direct oxidation of monophenolic compounds could generate *o*-quinone or *p*-quinone via four-electron and four-proton process [36,37]. However, this process can be suppressed by applying low overpotential [37]. Therefore, in this work, the observed oxidation peak could be attributed to the anodic oxidation of the aromatic ring in BPA and the formation of phenoxonium ions (compound II) via a two-electron and two-proton

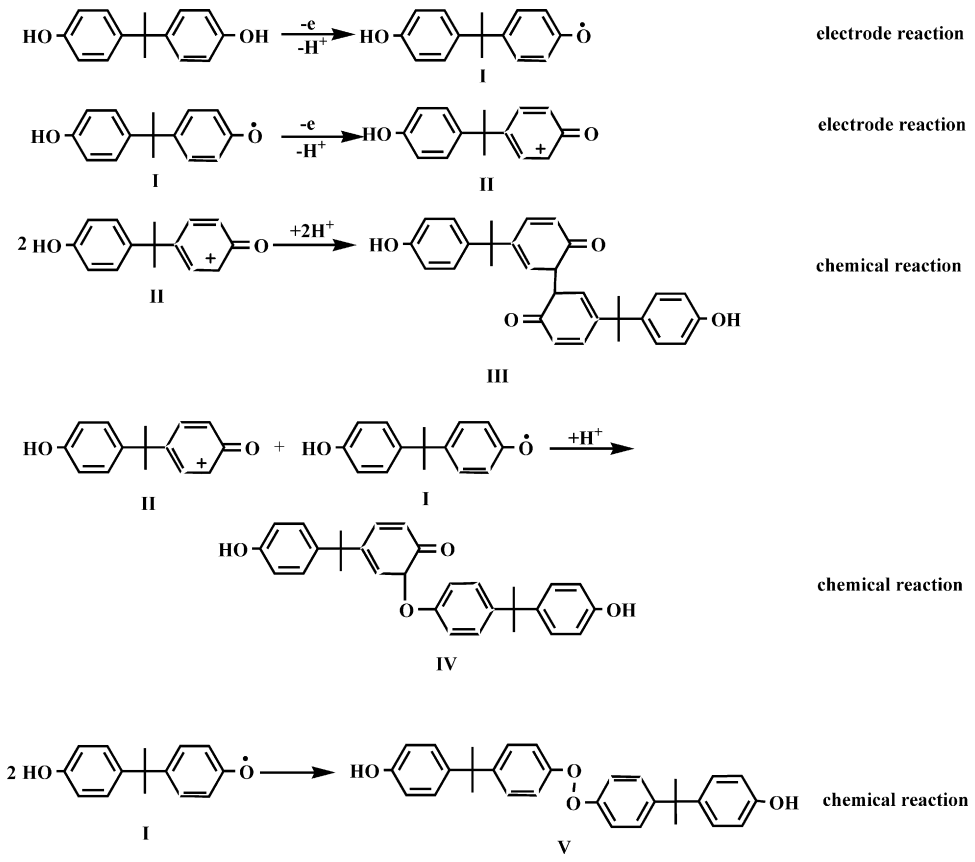

Scheme 1. The possible oxidation mechanism of BPA at PAMAM/CoTe/GCE.

process [33,35]. This is then followed by C—O, C—C and/or O—O coupling to form a neutral dimmer.

3.5. Effect of accumulation time

Fig. 5 illustrated the relationship between the oxidation peak current of BPA and accumulation time under open-circuit condition. With accumulation time increasing from 0 to 240 s, the oxidation peak current of 0.25 mM BPA gradually increased at PAMAM/CoTe/GCE. As extending accumulation time, the amount of BPA that accumulated at electrode surface also increased. Thus, the oxidation peak current of BPA increased. However, the peak current increased very slightly as accumulation time was longer than 240 s, which could be attributed to saturated adsorption of BPA at electrode surface. Considering both sensitivity and working efficiency, 240 s was chosen as the optimal accumulation time.

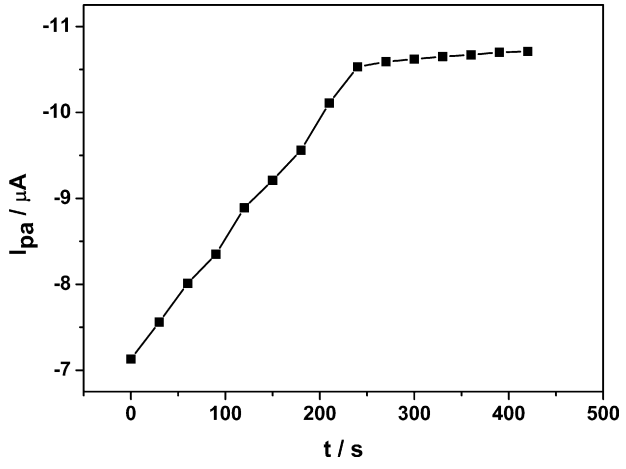

Fig. 5. Effect of accumulation time on the oxidation peak current of 0.25 mM BPA.

3.6. Chronocoulometry

The electrochemically effective surface areas of bare GCE and PAMAM/CoTe/GCE were determined by chronocoulometric method according to the formula given by Anson [38]:

$$Q(t) = \frac{2nFAcD^{1/2}t^{1/2}}{\pi^{1/2}} + Q_{dl} + Q_{ads} \quad (2)$$

where A is surface area of working electrode, c is concentration of substrate, D is diffusion coefficient, Q_{dl} is double layer charge which can be eliminated by background subtraction, Q_{ads} is Faradaic charge. Other symbols have their usual meanings. Based on the slope of the linear relationship between Q and $t^{1/2}$, A can be calculated when c, D and n are known. This experiment was carried out in 0.1 mM $K_3[Fe(CN)_6]$ solution containing 1 mM KCl, where the diffusion coefficient of $K_3[Fe(CN)_6]$ is 7.6×10^{-6} cm^2 s^{-1} [39]. According to the experiment results (shown in Fig. 6A), A was calculated to be 0.053 cm^2 and 0.21 cm^2 for GCE and PAMAM/CoTe/GCE, respectively. These results indicated that the electrode effective surface area was increased obviously after electrode modification, which would enhance the current response and decrease the detection limit.

The diffusion coefficient D and Faradic charge Q_{ads} of BPA at PAMAM/CoTe/GCE can also be determined by chronocoulometry based on Eq. (2). As shown in the insert of Fig. 6B, after background subtraction, the plot of Q against $t^{1/2}$ showed a linear relationship. The slope was 1.44×10^{-5} C s$^{1/2}$ and the intercept (Q_{ads}) was 9.67×10^{-7} C. As $n = 2$, $A = 0.21$ cm^2, and $c = 0.25$ mM, D

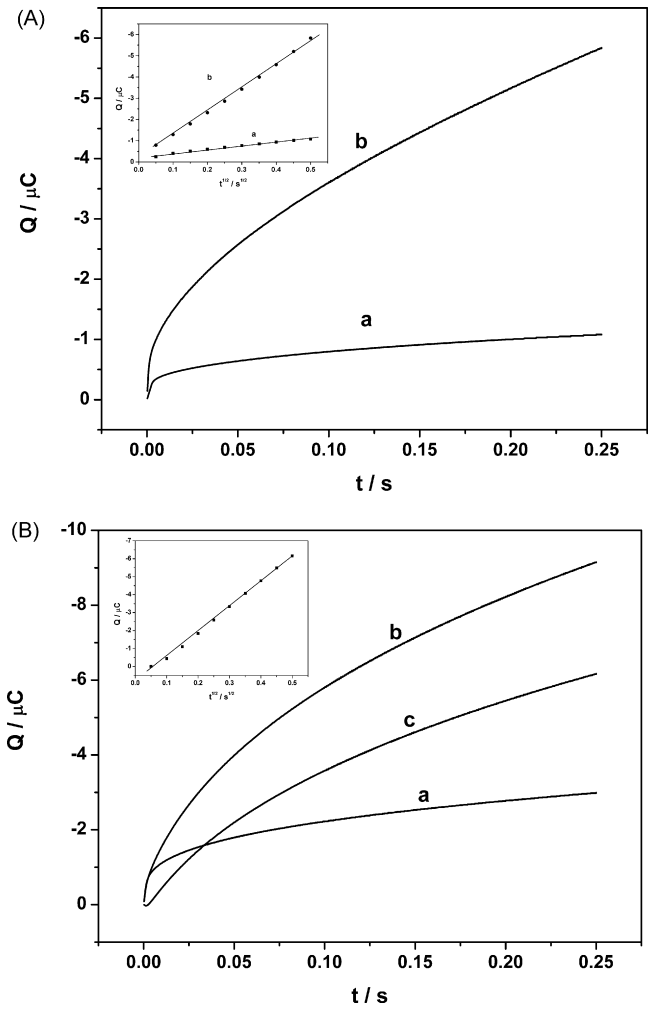

Fig. 6. (A) Plot of Q–t curves of GCE (a) and PAMAM/CoTe/GCE (b) in 0.1 mM $K_3[Fe(CN)_6]$ containing 1 M KCl. Insert: Plot of Q–$t^{1/2}$ curves on GCE (a) and PAMAM/CoTe/GCE (b). (B) Plot of Q–t curves of the modified electrode in 0.1 M pH 8.0 PBS in the absence (a) and presence (b) of 0.25 mM BPA. (c) Q–t curve after background subtracted. Insert: Plot of Q–$t^{1/2}$ curve on PAMAM/CoTe/GCE after background subtracted.

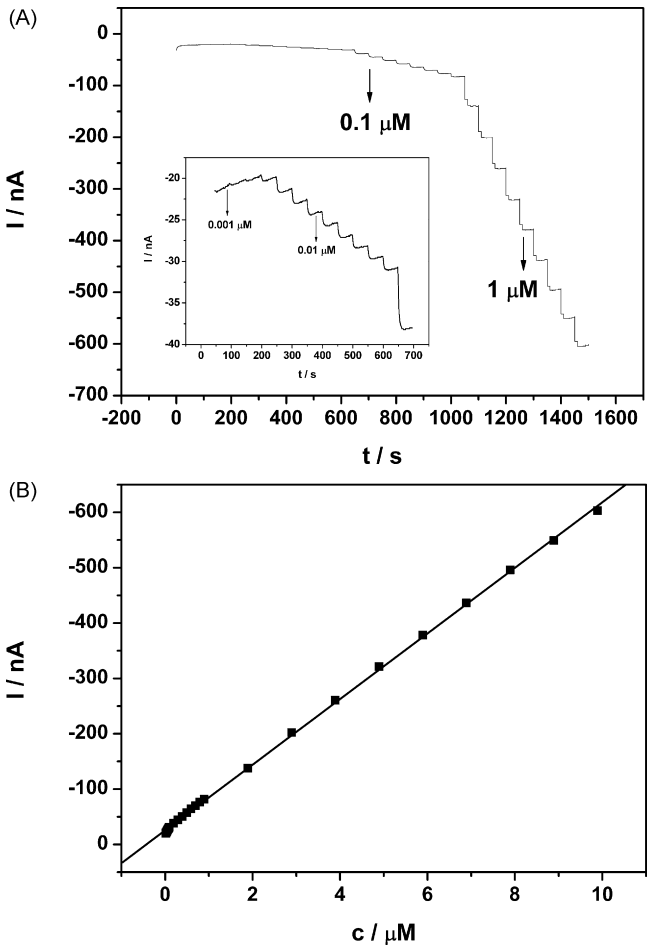

Fig. 7. (A) Typical current–time curve of PAMAM/CoTe/GCE upon the successive addition of 0.001, 0.01, 0.1 and 1 μM BPA into acutely stirred 0.1 M pH 8.0 PBS. Applied potential: 0.49 V. Insert: The magnified curve from 50 to 700 s. (B) Calibration curve.

was calculated to be 1.62×10^{-6} cm^2 s^{-1}. According to the equation $Q_{ads} = nFA\Gamma_s$, the adsorption capacity, Γ_s, can be obtained as 2.41×10^{-11} mol cm^{-2}.

3.7. Standard heterogeneous rate constant (k_s)

The standard heterogeneous rate constant (k_s) for totally irreversible oxidation of BPA at the modified electrode was calculated based on Eq. (3) [40]:

$$k_s = 2.415 \exp\left(\frac{-0.02F}{RT}\right) D^{1/2}(E_p - E_{p/2})^{-1/2} v^{1/2} \quad (3)$$

where E_p and $E_{p/2}$ represent the peak potential and the potential at which $I = I_p/2$ in linear sweep voltammetry (LSV), respectively. Other symbols have their usual meanings. In this experiment, $E_p = 489$ mV, $E_{p/2} = 431$ mV, $D = 1.62 \times 10^{-6}$ cm^2 s^{-1}, $v = 100$ mV s^{-1}, and $T = 298$ K. Therefore, k_s was calculated to be 1.85×10^{-3} cm s^{-1}.

3.8. Amperomatric response

Fig. 7 showed a typical current–time plot of PAMAM/CoTe/GCE under the optimized experimental conditions after successive addition of 0.001 μM, 0.01 μM, 0.1 μM and 1 μM of BPA to 0.1 M pH 8.0 PBS under magnetic stirring. The modified electrode can achieve the steady-state current within less than 5 s, which is a very rapid response to the change of BPA concentration. As shown in Fig. 7B, the current response was linear with BPA concentration in the range from 0.013 to 9.893 μM and the regression equation could be expressed as $I = -59.27c - 25.58$ (nA, μM, $R = 0.9998$). The detection limit was estimated to be 1×10^{-9} M (S/N = 3). And the detection limit in this work was lower than that of some other BPA sensors, such as tyrosinase/poly(thionine)/GCE (23 μM) [13], tyrosinase/boron-doped diamond electrode (1 μM) [14], tyrosinase-MWCN paste electrode (1 μM) [15], tyrosinase-CPE (0.15 μM) [41], tyrosinase-CPE (0.1 μM) [15], MCM-41/CPE (0.038 μM), tyrosinase-SWCN paste electrode (0.02 μM) [15], CoPc-CPE (0.01 μM) [12] and dsDNA/Au (0.01 μM) [42] and carbon paste electrode (0.0075 μM) [24], indicating that this proposed method could potentially be used to sensitively monitor BPA concentration. The lower detection limit could be ascribed to the electrocatalytic activity of CoTe and the accumulation ability of protonated PAMAM.

3.9. Reproducibility, stability and interference

The fabrication reproducibility was investigated in 0.1 μM BPA with RSD of 4.86% for five different electrodes. The stability of PAMAM/CoTe/GCE was also investigated by measuring the current response of 0.1 μM BPA. Between measurements, the electrode was stored at 4°C in a refrigerator. The current retained 93% of its orig-

Table 1
Determination of BPA in water samples.

Type of water[a]	Added (μM)	Found[b] (μM)	RSD[c] (%)	Recovery (%)
River	0.100	0.097	3.78	97.00
Lake	0.100	0.103	3.86	103.0
Waste	0.500	0.536	5.52	107.2
Tap water	1.000	0.982	2.45	98.20

[a] All water samples were collected from Taian, Shandong Province, China.
[b] Mean of five measurements.
[c] Relative standard deviation for $n = 5$.

inal response after 10 days, while the current response decreased to 88% and 81% after 15 and 25 days, respectively. The electrode still retained 72% of its original response even after 35 days. The phenomenon indicated the good stability of PAMAM/CoTe/GCE.

To evaluate the selectivity of the fabricated electrode, the influence of some common phenolic complexes and inorganic ions were examined in PBS solution (pH 8.0) containing 1 μM BPA. The results suggested that 100-fold concentration of phenol, hydroquinone, hydroxyphenol, pyrocatechol, 4-nitrophenol and 2,4-dinitrophenol had no influence on the signals of BPA with deviations below 10%. Additionally, some inorganic ions such as 400-fold concentration of Na^+, Ca^{2+}, Mg^{2+}, Fe^{3+}, Al^{3+}, Zn^{2+}, Cu^{2+}, Cl^-, $SO_4{}^{2-}$, $PO_4{}^{3-}$ and $NO_3{}^-$ had no influence on BPA determination.

The results obtained from reproducibility, stability and interference tests indicated that PAMAM/CoTe/GCE might be suitable for practical application.

3.10. Practical application

In order to evaluate the performance of PAMAM/CoTe/GCE in practical analytical application, the determination of BPA in real matrix samples were checked via a recovery study according to the above-described analytical procedure. As can be seen from Table 1, the results obtained in determination of BPA in water samples (river, lake, waste water and tap water) were good. In fact, the recoveries ranged from 97.0% to 107.2%. Therefore, PAMAM/CoTe/GCE is able to predict the concentration of BPA in real matrix samples.

4. Conclusion

The present study shows that the electrochemical determination of BPA using PAMAM/CoTe/GCE is a suitable strategy for determination of trace amounts of this compound in natural water. The oxidation peak current of BPA was significantly enhanced and the oxidation overpotential was decreased after electrode modification. The reason can be attributed to the catalytic activity of CoTe, and the high adsorption capacity and conductivity of positively charged PAMAM. The proposed method was successfully applied in determining BPA in real water samples with recovery ranging from 97.0% to 107.2%. Compared with other electrochemical methods, this new method possesses lower oxidation potential, higher sensitivity, lower detection limit and faster response.

Acknowledgements

This work was supported by the National Natural Science Foundation of China (No. 20775044) and the Natural Science Foundation of Shandong province, China (Y2006B20).

References

[1] A. Krishnan, P. Stathis, S. Permuth, L. Tokes, D. Feldman, Bisphenol-A: an estrogenic substance is released from polycarbonate flasks during autoclaving, Endocrinology 132 (1993) 2279–2286.
[2] M. Munoz-de-Toro, C. Markey, P. Wadia, E. Luque, B. Rubin, C. Sonnenschein, A. Soto, Perinatal exposure to bisphenol-A alters peripubertal mammary gland development in mice, Endocrinology 146 (2005) 4138–4147.
[3] A. Goodson, H. Robin, W. Summerfield, I. Cooper, Migration of bisphenol A from can coatings—effects of damage, storage conditions and heating, Food Addit. Contam. 21 (2004) 1015–1026.
[4] J. Lopez-Cervantes, P. Paseiro-Losada, Determination of bisphenol A in, and its migration from, PVC stretch film used for food packaging, Food Addit. Contam. 20 (2003) 596–606.
[5] X.L. Cao, J. Corriveau, Migration of Bisphenol A from polycarbonate baby and water bottles into water under severe conditions, J. Agric. Food Chem. 56 (2008) 6378–6381.
[6] M. Telscher, U. Schuller, B. Schmidt, A. Schaffer, Occurrence of a nitro metabolite of a defined nonylphenol isomer in soil/sewage sludge mixtures, Environ. Sci. Technol. 39 (2005) 7896–7900.
[7] Y. Watabe, T. Kondo, M. Morita, N. Tanaka, J. Haginaka, K. Hosoya, Determination of bisphenol A in environmental water at ultra-low level by high-performance liquid chromatography with an effective on-line pretreatment device, J. Chromatogr. A 1032 (2004) 45–49.
[8] M. Kawaguchi, K. Inoue, M. Yoshimura, R. Ito, N. Sakui, N. Okanouchi, H. Nakazawa, Determination of bisphenol A in river water and body fluid samples by stir bar sorptive extraction with in situ derivatization and thermal desorption-gas chromatography–mass spectrometry, J. Chromatogr. B 805 (2004) 41–48.
[9] A. Ballesteros-Gómez, S. Rubio, D. Pérez-Bendito, Analytical methods for the determination of bisphenol A in food, J. Chromatogr. A 1216 (2009) 449–469.
[10] Y. Kanekiyo, R. Naganawa, H. Tao, Molecular imprinting of bisphenol A and alkylphenols using amylose as a host matrix, Chem. Commun. 2002 (2002) 2698–2699.
[11] F. Wang, J. Yang, K. Wu, Mesoporous silica-based electrochemical sensor for sensitive determination of environmental hormone bisphenol A, Anal. Chim. Acta 638 (2009) 23–28.
[12] H. Yin, Y. Shout, S. Ai, Preparation and characteristic of cobalt phthalocyanine modified carbon paste electrode for bisphenol A detection, J. Electroanal. Chem. 626 (2009) 80–88.
[13] E. Dempsey, D. Diamond, A. Collier, Development of a biosensor for endocrine disrupting compounds based on tyrosinase entrapped within a poly (thionine) film, Biosens. Bioelectron. 20 (2004) 367–377.
[14] H. Notsu, T. Tatsuma, A. Fujishima, Tyrosinase-modified boron-doped diamond electrodes for the determination of phenol derivatives, J. Electroanal. Chem. 523 (2002) 86–92.
[15] D. Mita, A. Attanasio, F. Arduini, N. Diano, V. Grano, U. Bencivenga, S. Rossi, A. Amine, D. Moscone, Enzymatic determination of BPA by means of tyrosinase immobilized on different carbon carriers, Biosens. Bioelectron. 23 (2007) 60–65.
[16] W.J.R. Santos, P.R. Lima, A.A. Tanaka, S. Tanaka, L.T. Kubota, Determination of nitrite in food samples by anodic voltammetry using a modified electrode, Food Chem. 113 (2009) 1206–1211.
[17] Z. Wang, Q. Xu, H.-Q. Wang, Q. Yang, J.-H. Yu, Y.-D. Zhao, Hydrogen peroxide biosensor based on direct electron transfer of horseradish peroxidase with vapor deposited quantum dots, Sens. Actuator B 138 (2009) 278–282.
[18] Q. Liu, X. Lu, J. Li, X. Yao, Direct electrochemistry of glucose oxidase and electrochemical biosensing of glucose on quantum dots/carbon nanotubes electrodes, Biosens. Bioelectron. 22 (2007) 3203–3209.
[19] G. Li, X. Li, J. Wan, S. Zhang, Dendrimers-based DNA biosensors for highly sensitive electrochemical detection of DNA hybridization using reporter probe DNA modified with Au nanoparticles, Biosens. Bioelectron. 24 (2009) 3281–3287.
[20] Q. Chen, S. Ai, X. Zhu, H. Yin, Q. Ma, Y. Qiu, A nitrite biosensor based on the immobilization of cytochrome *c* on multi-walled carbon nanotubes-PAMAM-chitosan nanocomposite modified glass carbon electrode, Biosens. Bioelectron. 24 (2009) 2991–2996.
[21] Z. Liu, Y. Yang, H. Wang, Y. Liu, G. Shen, R. Yu, A hydrogen peroxide biosensor based on nano-Au/PAMAM dendrimer/cystamine modified gold electrode, Sens. Actuator B 106 (2005) 394–400.
[22] W. Chen, D. Tomalia, J. Thomas, Unusual pH-dependent polarity changes in PAMAM dendrimers: evidence for pH-responsive conformational changes, Macromolecules 33 (2000) 9169–9172.
[23] H. Fan, Y. Zhang, M. Zhang, X. Wang, Y. Qian, Glucose-assisted synthesis of CoTe nanotubes in situ templated by Te nanorods, Cryst. Growth Des. 8 (2008) 2838–2841.
[24] W. Huang, Voltammetric determination of bisphenol A using a carbon paste electrode based on the enhancement effect of cetyltrimethylammonium bromide (CTAB), Bull. Korean Chem. Soc. 26 (2005) 1560–1564.
[25] S. Tanaka, Y. Nakata, T. Kimura, M. Kawasaki, H. Kuramitz, Electrochemical decomposition of bisphenol A using Pt/Ti and SnO_2/Ti anodes, J. Appl. Electrochem. 32 (2002) 197–201.
[26] H. Kuramitz, M. Matsushita, S. Tanaka, Electrochemical removal of bisphenol A based on the anodic polymerization using a column type carbon fiber electrode, Water Res. 38 (2004) 2331–2338.
[27] D. Vega, L. Agüí, A. González-Cortés, P. Yáñez-Sedeño, J.M. Pingarrón, Electrochemical detection of phenolic estrogenic compounds at carbon nanotube-modified electrodes, Talanta 71 (2007) 1031–1038.
[28] L. Agüí, P. Yáñez-Sedeño, J.M. Pingarrón, Preparation and characterization of a new design of carbon-felt electrode for phenolic endocrine disruptors, Electrochim. Acta 51 (2006) 2565–2571.

[29] L. Tang, Y. Zhu, L. Xu, X. Yang, C. Li, Amperometric glutamate biosensor based on self-assembling glutamate dehydrogenase and dendrimer-encapsulated platinum nanoparticles onto carbon nanotubes, Talanta 73 (2007) 438–443.
[30] M. Murugananthan, S. Yoshihara, T. Rakuma, T. Shirakashi, Mineralization of bisphenol A (BPA) by anodic oxidation with boron-doped diamond (BDD) electrode, J. Hazard. Mater. 154 (2008) 213–220.
[31] T. Luckza, Preparation and characterization of the dopamine film electrochemically deposited on a gold template and its applications for dopamine sensing in aqueous solution, Electrochim. Acta 53 (2008) 5725–5731.
[32] E. Laviron, Adsorption, autoinhibition and autocatalysis in polarography and in linear potential sweep voltammetry, J. Electroanal. Chem. 52 (1974) 355–393.
[33] M. Ngundi, O. Sadik, T. Yamaguchi, S. Suye, First comparative reaction mechanisms of β-estradiol and selected environmental hormones in a redox environment, Electrochem. Commun. 5 (2003) 61–67.
[34] H. Kuramitz, Y. Nakata, M. Kawasaki, S. Tanaka, Electrochemical oxidation of bisphenol A. Application to the removal of bisphenol A using a carbon fiber electrode, Chemosphere 45 (2001) 37–43.
[35] H. Eickhoff, G. Jung, A. Rieker, Oxidative phenol coupling-tyrosine dimers and libraries containing tyrosyl peptide dimers, Tetrahedron 57 (2001) 353–364.
[36] M. Ferreira, H. Varela, R.M. Torresi, G. Tremiliosi-Filho, Electrode passivation caused by polymerization of different phenolic compounds, Electrochim. Acta 52 (2006) 434–442.
[37] L. Papouchado, R.W. Sandford, G. Petrie, R.N. Adams, Anodic oxidation pathways of phenolic compounds. Part 2. Stepwise electron transfers and coupled hydroxylations, J. Electroanal. Chem. 65 (1975) 275–284.
[38] F. Anson, Application of potentiostatic current integration to the study of the adsorption of cobalt (III)-(ethylenedinitrilo (tetraacetate)) on mercury electrodes, Anal. Chem. 36 (1964) 932–934.
[39] R. Adams, Electrochemistry at Solid Electrodes, M. Dekker, New York, 1969.
[40] J. Velasco, Determination of standard rate constants for electrochemical irreversible processes from linear sweep voltammograms, Electroanalysis 9 (1997) 880–882.
[41] S. Andreescu, O. Sadik, Correlation of analyte structures with biosensor responses using the detection of phenolic estrogens as a model, Anal. Chem. 76 (2004) 552–560.
[42] F. Yan, O. Sadik, Enzyme-modulated cleavage of dsDNA for supramolecular design of biosensors, Anal. Chem. 73 (2001) 5272–5280.